Comparing the Penman-Monteith equation and a modified Jarvis-Stewart model with an artificial neural network to estimate stand-scale transpiration and canopy conductance

Rhys Whitley[a,b,c] , Belinda Medlyn[d], Melanie Zeppel[a,c], Catriona Macinnis-Ng[a,c], Derek Eamus[a,c,†]

[a]*Institute for Water and Environmental Resource Management, University of Technology Sydney, PO Box 123, Broadway, NSW 2007, Australia*

[b]*Department of Physics and Advanced Materials, University of Technology Sydney, PO Box 123, Broadway, NSW 2007, Australia*

[c]*Department of Environmental Science, University of Technology Sydney, PO Box 123, Broadway, NSW 2007, Australia*

[d]*Department of Biological Sciences, Macquarie University, NSW 2109, Australia.*

[†]*Corresponding author: Tel: (+61-2) 9514-2203; Fax: (+61-2) 9514-2219; Email address: rhys.j.whitley@uts.edu.au*

ABSTRACT

The responses of canopy conductance to variation in solar radiation, vapour pressure deficit and soil moisture have been extensively modelled using a Jarvis-Stewart (JS) model. Modelled canopy conductance has then often been used to predict transpiration using the Penman-Monteith (PM) model. We previously suggested an alternative approach in which the JS model is modified to

directly estimate transpiration rather than canopy conductance. In the present study we used this alternative approach to model tree water fluxes from an Australian native forest over an annual cycle. For comparative purposes we also modelled canopy conductance and estimated transpiration *via* the PM model. Finally we applied an artificial neural network as a statistical benchmark to compare the performance of both models. Both the PM and modified JS models were parameterised using solar radiation, vapour pressure deficit and soil moisture as inputs with results that compare well with previous studies. Both models performed comparably well during the summer period. However, during winter the PM model was found to fail during periods of high rates of transpiration. In contrast, the modified JS model was able to replicate observed sapflow measurements throughout the year although it too tended to underestimate rates of transpiration in winter under conditions of high rates of transpiration. Both approaches to modelling transpiration gave good agreement with hourly, daily and total sums of sapflow measurements with the modified JS and PM models explaining 87% and 86% of the variance respectively. We conclude that these three approaches have merit at different time-scales.

Keywords: Canopy conductance, nocturnal flows, transpiration, Jarvis-Stewart model

1. Introduction

Water flux through trees is a principal pathway for the discharge of soil water. Consequently, to determine the water budget of woody landscapes, tree canopy water fluxes must be known, either through direct measurement or through modelling (Komatsu et al., 2006a; Wullschleger et al., 2006; Rollenbeck and Dieter, 2007; Simonin et al., 2007). Canopy conductance, solar radiation, vapour

pressure deficit and soil moisture are the major determinants of the rate of water flux through trees (Jarvis and McNaughton, 1986; Wullschleger et al., 2001; Zeppel, 2006; Zeppel and Eamus, 2008; Zeppel et al., 2008) and seasonal variations in these three abiotic variables cause seasonal variation of canopy transpiration per unit ground area (E_c) and canopy conductance (g_c) (Harris et al., 2004; Komatsu et al., 2006b). Measuring seasonal variations of these abiotic variables and parameterising their impact on E_c, is important for quantifying intra-annual variation in E_c. In this study we investigated how variations in the driving variables impact g_c and E_c in order to develop a model of seasonal variability in E_c for an Australian native woodland.

The regulation of canopy conductance and transpiration has received extensive investigation (Jarvis, 1976; Stewart, 1988; Granier and Loustau, 1994; Harris et al., 2004; Komatsu et al., 2006b). Such studies use measured values of sapflow or eddy covariance and an inversion of the Penman-Monteith (PM) equation to derive measurements of g_c. In most applications of the PM equation, the JS model (Jarvis, 1976; Stewart, 1988) is also required to quantify a set of seasonal response terms describing the functional relationships among g_c, R_s, D and θ, to give modelled predictions of g_c, as needed in the PM equation. This approach has been applied to poplar trees, maritime pine forest, oak forest, spruce and pine forests, an Amazonian pasture and rainforest, and a Japanese conifer forest (Gash et al., 1989; Dolman et al., 1991; Ogink-Hendriks, 1995; Wright et al., 1995; Zhang et al., 1997; Lagergren and Lindroth, 2002; Sommer et al., 2002; Harris et al., 2004; Komatsu et al., 2006a, b). However, one problem in applying JS models is the requirement for a large degree of spatial and temporal replication in either stomatal conductance or g_c, and subsequent use of the PM equation in order to calculate transpiration rate. Furthermore, the PM equation is known to predict E_c poorly under limiting soil moisture conditions and it may correlate with observation best when E_c is large (David et al., 1997; Rana et al., 2005).

The PM equation (Monteith, 1965) is commonly used to estimate evapotranspiration of crops (Yunusa et al., 2000; Lu et al., 2003) and forests (Gash et al., 1989; Kosugi et al., 2007; Zeppel and Eamus, 2008). In the past decade the PM equation has been simplified (Granier et al., 1996; Whitehead, 1998; Granier et al., 2000; Ewers et al., 2007). For a well-coupled forest, where transpiration is controlled by stomatal aperture in response to meteorological changes, E_c can be calculated from g_c and D because $E_c = g_c D$. Since $g_c = g_s LAI$, where LAI is leaf area index and g_s is stomatal conductance (Whitehead, 1998) and if we assume a negligible effect of aerodynamic conductance on transpiration (that is, aerodynamic conductance is much greater than g_c), then we can re-express the PM equation for g_s as a function of its driving environmental variables and LAI (Jarvis, 1976; Whitehead, 1998).

$$E_c = LAI.g_{s\max} f(R_s) f(\theta) f(D) D \quad (1)$$

where, $g_{s,max}$ denotes the maximum stomatal conductance under non-limiting environmental conditions and f denotes a series of normalised functions which will be described in the next section. Equation (1) can be estimated using the non-linear, multiplicative, independent functions originally described by Jarvis (1976), discussed by Whitehead (1998) and subsequently widely applied (Wright et al., 1995, Harris et al., 2004; Komatsu et al., 2006a, b). The above formulation is functionally equivalent to the PM equation, yet is much simpler to fit, requires fewer measurements and specifically avoids the circularity of inverting the PM, as applied in the past (Ewers and Oren, 2000; Lu et al., 2003; Pataki and Oren, 2003).

Parameterisation of a JS model over an annual cycle for Australian native woodlands and forests has not yet been conducted, to our knowledge. Stomatal conductance and transpiration responses to D

have been investigated for northern Australian savannas by Thomas and Eamus (1999), Thomas et al. (2000) and Eamus and Shanahan (2002) and soil moisture responses of E_c and g_c have been investigated (Hutley et al., 2001; Zeppel and Eamus, 2008; Zeppel et al., 2008). In previous work (Whitley et al., 2008) we modified the JS model to estimate E_c directly, thereby avoiding the PM equation and showed that it is possible to estimate E_c empirically from only 3 driving variables. However, the study utilised a 30 day period and it was unclear as to whether the model could be applied across different seasons where much larger variations in R_s, D and θ occur. In this paper we scale estimates of stand water use from a larger study that encompasses a much larger range of climate and soil moisture variability to examine whether the modified JS model requires single or multiple parameterisations when using multi-season data. JS models have been used extensively because of their simplicity and they allow calculation of g_c as a function of meteorological variables and soil moisture content (Jarvis, 1976; Wright et al., 1995; Whitehead, 1998; Harris et al., 2004; Komatsu et al., 2006a, b; Ewers et al., 2007).

We present the results from a field campaign that measured soil moisture content, net radiation, tree water use, vapour pressure deficit and leaf area index, with the primary goal of scaling vegetation water use without the need to measure either g_s or g_c and without, therefore, use of the PM equation. We also investigate intra-annual variability of E_c and g_c to seasonal variation of the driving environmental variables. In order to measure the performance of our transpiration model, we incorporate the use of an artificial neural network (ANN) as a statistical benchmark to which our modified JS model and PM equation are compared. Finally, we compare our results from this study with those found in previous literature studies to show the spatial variability of models parameterised over different sites and ecosystems.

2. Methods

2.1. Site description

A remnant open woodland site located approximately 70 km south of Tamworth, in north-western NSW (31.5 ° S, 150.7 ° E, elevation 390 m), was used in this study. A full description of the site is provided in Zeppel et al. (2004) and Zeppel and Eamus (2008). In summary, the average height of the trees was 15 m and is dominated by *Eucalyptus crebra* and *Callitris glaucophylla*. These two species contributed approximately 75% of the tree basal area at the site. Total tree basal area was 23.8 ± 3.4 m^2 ha^{-1}. The eucalypts had a lower density than the *Callitris* (42 stems ha^{-1} compared to 212 stem ha^{-1}) but contributed most (approximately 75 %) to the basal area of the two species combined because its average diameter was much larger than that of the *Callitris*. The understorey was dominated by grasses, predominantly *Stipa* and *Aristada* species. Soils at the site were shallow with well-drained acid lithic bleached earthy sands (Banks, 1998) with occasional exposed sandstone.

Incoming solar radiation and wet and dry bulb temperature were measured at hourly intervals at a weather station located in a cleared pasture (> 4 ha) approximately 100 m from the remnant woodland. Wind speed was measured with a cup anemometer situated about 3 m above the canopy and soil moisture was measured with Theta Probes (Delta-T Devices, UK) at 50 cm depth at two locations. Leaf area index was measured at seven locations in the woodland, as previously described (Zeppel, 2006) using a Li-Cor 2000 Plant Canopy Analyser, four times during the year of study (2004). LAI ranged from 0.9 to 1.0 on these four occasions (data not shown).

142 *2.2. Water use by individual trees*

143

144 The rate of water use by individual trees (L d^{-1}) was measured at 15 minute intervals using sapflow
145 sensors (model SF100, Greenspan Technology, Pty Ltd, Warwick, Australia) as previously described
146 (Zeppel et al., 2004). For each species 10-12 trees were chosen to sample the full range of tree sizes
147 and each tree was instrumented with 4 sensors. Sensors were stratified with depth (at 1/3 and 2/3 of
148 the depth) through the sapwood (Medhurst et al., 2002; Zeppel et al., 2004). Sapflows were corrected
149 for wound effects, sapwood area, radial variability in flow and volumetric fractions of water and
150 wood (Zeppel et al., 2004). Wound width was measured for both sensor sets in each of seven trees of
151 both species (O'Grady et al. 1999), at the end of the sampling period. A wound width of 2.5 mm for
152 *C. glaucophylla* and 3.7 mm for *Eucalyptus crebra* was used to correct velocity estimates. Basal area
153 and diameter at breast height (DBH) of all trees were measured in 7 replicate 50 m x 50 m plots
154 (Zeppel et al., 2004).

155

156 *2.3. Scaling to stand transpiration*

157

158 Scaling from individual trees to stand transpiration was done by multiplying the average hourly sap
159 velocity (SV_{plot}) by the sapwood area per unit ground area (SA_{plot}); further details of this can be found
160 in Zeppel et al. (2004) and Whitley et al. (2008). SA_{plot} was calculated from measurements of
161 sapwood depth for both tree species and from plot-level measurements of the stand. Each 24 hour
162 period was summed to give the daily sap flux (cm^3 d^{-1} $plot^{-1}$).

163

164 The water use (cm^3 water d^{-1} $plot^{-1}$) of each plot (with an area of 2500 m^2) was converted to stand
165 transpiration (mm^3 of water d^{-1} mm^{-2} ground area). The DBH of all trees in 7 replicate plots was

166 measured and therefore there were 7 estimates of stand water use (cm^3 sap flux day^{-1} cm^{-2} ground
167 area) for each day. The mean and standard error of all 7 plots, for each day, was then estimated, and
168 converted from cm^3 water d^{-1} cm^{-2} ground area to yield stand water use (E_c^{stand} , mm hr^{-1}).
169
170 *2.4. Modelling*
171
172 Our goals for this analysis were threefold. First, to parameterise two models in order to derive a set of
173 seasonal response terms describing the responses of E_c and g_c to changes in their driving
174 environmental variables. Second, to compare outputs of modelled E_c via a modified JS model as
175 defined by Whitley et al. (2008) and from the PM equation. Finally, we quantify the performance of
176 these models statistically by comparing outputs of the PM equation (E_c^{PM}) and the modified JS
177 model (E_c^{JS}), against that of an artificial neural network (ANN). We now outline the two models
178 used in this study and then describe the ANN applied to the data.
179
180 *2.4.1. The Penman-Monteith model*
181
182 An inversion of the PM equation (Eq.2) was solved in order to derive measurements for canopy
183 conductance (g_c, mm s^{-1}).

184
$$g_c = \frac{\gamma \lambda E_c g_a}{\Delta R_n + k_t \rho C_p D g_a - \lambda(\Delta + \gamma) E_c} \qquad (2)$$

185 where Δ is the slope of the relationship between the saturation vapour pressure and temperature (kPa
186 $^oC^{-1}$), R_n is the net radiation above the forest canopy (MJ m^{-2} hr^{-1}), k_t is a conversion factor (3600 s h^{-1}
187 for E_c in mm hr^{-1}), ρ is the air density (kg m^{-3}), C_p is the specific heat of air (1.013 MJ kg-1 $^oC^{-1}$), g_a

188 is the aerodynamic conductance (m s^{-1}), γ is the psychometric constant (0.066 kPa $^{o}C^{-1}$) and λ is the
189 latent heat of vaporisation (2.39 MJ kg^{-1}). g_c was modelled according to the JS approach,
190
191 $$g_c^{mod} = g_{c\,max} f_1(R_s) f_2(D) f_3(\theta) \quad (3)$$
192
193 using a set of functional forms via the relationships between g_c and its three driving environmental
194 variables; volumetric soil moisture content (θ, %), solar radiation levels (R_s, W m^{-2}) and vapour
195 pressure deficit (D, kPa). Scaling from leaf to canopy level and *vice versa* was achieved by including
196 a *LAI* term, incorporated via the $g_{c,max}$ term such that $g_{c,max} = g_{s,max} LAI$. g_c^{mod} was subsequently used
197 in equation (1) in order to derive estimates of E_c^{PM} .
198
199 *2.4.2. The modified Jarvis-Stewart model*
200
201 Following the formulation and theory for an aerodynamically well-coupled forest (Jarvis and
202 McNaughton (1986)) given by Equation (1), two modifications were made to Equation (3) to develop
203 our second model. First, E_c was modelled directly; rather than following the complicated process
204 described for application of the PM model to calculate E_c, we express E_c in the same way as g_c, as
205 defined by Jarvis (1976) and Stewart (1988). E_c was expressed as function of R_s, D and θ, whereby
206 these functions act in the same way as in Equation (3) as a set of scaling terms that reduce a bulk
207 maximum stand transpiration term. Second, we define a new function $\hat{f}_2$ to explain the variation of
208 E_c with D. Thus, we express E_c^{JS} as,
209
210 $$E_c^{JS} = E_{c\,max} f_1(R_s) \hat{f}_2(D) f_3(\theta) \quad (4)$$

211 *2.5. Seasonal response functions*

212

213 The functions f_i are a set of scaling terms that reduce a bulk maximum value of stand transpiration
214 ($E_{c,max}$) and canopy conductance ($g_{c,max}$) in response to changes in R_s, D and θ. The functions f_i take
215 on values between 0 and 1, such that any changes in the values of R_s, D and θ will proportionally
216 modify the parameters $E_{c,max}$ and $g_{c,max}$ to give modelled estimates of E_c and g_c respectively. Hourly
217 estimates for stand water use (E_c, mm hr^{-1}) were determined from functions f_i. To determine the
218 response functions for E_c and g_c in terms of their driving environmental variables, it is assumed that
219 the responses to each driving variable are independent (Jarvis, 1976). The functional forms for R_s, D
220 and θ for this study are taken from Whitley et al. (2008) and based on those of Stewart (1988), Wright
221 et al. (1995) and Harris et al. (2004). Thus, the response functions for R_s and θ are,

222

223 $$f_1(R_S) = \left(\frac{R_s}{1000}\right)\left(\frac{1000 + k_1}{R_s + k_1}\right) \quad (5)$$

224

225 $$f_3(\theta) = \begin{cases} 0 & ,\theta < \theta_w \\ \dfrac{\theta - \theta_w}{\theta_c - \theta_w} & ,\theta_w < \theta < \theta_c \\ 1 & ,\theta > \theta_c \end{cases} \quad (6)$$

226 Equation (5) describes the radiation response, showing an asymptotic saturating function that plateaus
227 at approximately 1000 W m^{-2}, with k_1 (W m^{-2}) describing the curvature of the relationship.
228 Hyperbolic saturating functions describing R_s have been applied extensively at leaf, tree and canopy
229 scales for conductance (Kelliher et al., 1993; Granier et al., 2000) and for tree water use (Komatsu et
230 al., 2006b). Equation (6) shows the soil moisture response to be a three-phase relationship, where θ_w

231 and θ_c denote the points of inflection in the relationship and can loosely be termed "wilting point"
232 and "field capacity" respectively.
233
234 We express the functional response of g_c to D as traditionally defined by Jarvis (1976) and Stewart
235 (1988) as:
236 $$f_2(D) = \exp(-k_3 D) \quad (7a)$$
237 where, k_3 is a free parameter, describing the decrease in g_c with increasing D. If we follow the
238 relationship expressed in Equation (1), that $E_c = g_c D$, we can formulate a function $\hat{f}_2(D)$, for E_c as:
239
240 $$\hat{f}_2(D) = k_2 D \exp(-k_3 D) \quad (7b)$$
241
242 where, the parameters k_2 and k_3 describe the rate of change at low and high atmospheric demand. The
243 vapour pressure deficit function for E_c (Eq. 7b), is a new term and follows the shape of the Bolztmann
244 distribution function. However, this is not normalised as Equations (5), (6) and (7a) are, and some
245 care is needed during the optimisation. Examination of Equations (7a, b) shows that their response
246 functions replicate the three-phase response of transpiration to variation in g_s (Monteith, 1995;
247 Thomas and Eamus, 1999; Eamus and Shanahan, 2002).
248
249 *2.6. Model parameterisation*
250
251 The model was parameterised from experimental (measured) data using a genetic algorithm and
252 weighted least squares (WLS). A weighting term (σ_i) was incorporated to better quantify the
253 distribution of error in the measurements and hence ensure the optimised free parameters were closer
254 to maximum likelihood. The parameters ref_{max} ($E_{c,max}$ and $g_{c,max}$), k_1, k_2, k_3, θ_W and θ_C are the

optimised free parameters that represent response constants in the JS model. A multivariate optimisation for Equations (3) and (4) was done by minimising the weighted sum of the square of residuals (WSSR), given that k_1, k_2, k_3, θ_w and θ_c are set at some arbitrary starting values. We express the WSSR as:

$$\chi^2_{\min} = \sum_{i=1}^{N} \frac{(y_i - \hat{y}_i)^2}{\sigma_i^2} \quad (8a)$$

where

$$\sigma_i = \beta y_i \quad (8b)$$

y_i is the *i*th experimental value, $\hat{y}_i$ is the *i*th predicted value based on the equation fitted to the data, σ_i where '*i*' is the *i*th standard deviation and N is the number of data points. We assume the heteroscedasticity to be explained by Equation (8b), expressing the standard deviation to be proportional to the experimental data y_i, multiplied by an error constant of proportionality β (Kirkup et al., 2004). In order to specify whether σ_i is normally distributed, we have assumed that the residuals are a surrogate for σ_i such that $(y_i - \hat{y}_i) \equiv \sigma_i$. For this study we assume random measurement error (σ_i) to be normally distributed and heteroscedastic based on observations of the weighted residuals.

Difficulties in optimisation are commonly experienced when using a least squares criterion at large dimensionalities. As the problem moves from linear to non-linear, the parameter space very quickly becomes increasingly difficult to optimise and therefore it is increasingly difficult to yield parameter values that are maximum likelihood. Where local minima occur, these cause early convergence over

277 the large parameter space, hampering the optimisation. To overcome these problems, we incorporated
278 a genetic algorithm instead of the traditional Levenberg-Marquardt or Gauss-Newton algorithms.
279 Unlike the gradient descent methods, a genetic algorithm is able to cover the entire parameter space
280 with a large set of possible solutions. These solutions evolve and undergo a simulated process of
281 natural selection until the best solution and hence the global minima equating to parameter values that
282 are maximum likelihood, is found. A more detailed explanation of genetic algorithms and their design
283 can be found in Goldberg (1989). For this study we used a pre-built genetic algorithm package in the
284 *Mathematica*© software called Differential Evolution. The cross probability (probability of mating)
285 was set to 50%, while population size was set automatically by the algorithm and run for 100,000
286 iterations to give an adequate amount of generations to find the global maxima.
287
288 *2.7. Artificial neural network*
289
290 In order to test the modified JS model and PM equation against some form of statistical benchmark,
291 we used an artificial neural network (ANN) as a comparator (Kohanen, 1989; Hsu et al., 2002;
292 Abramowitz, 2005). A multivariate ANN procedure called a Self-Organising Linear Output map
293 (SOLO) developed by Hsu et al. (2002) was used for this study. SOLO learns the relationship
294 between inputs and outputs through the use of a training data set. Input information (R_s, D and θ)
295 classified in a Self Organising Feature Map (SOFM) (Kohanen, 1989). This classifies the driving
296 variables into groups or 'nodes' of some arbitrary matrix size defined by the user. This results in a set
297 of nodes describing the input and output space. A linear regression is then performed between nodes
298 of both spaces resulting in an approximation of our output variable E_c^{ANN}. The ANN is a purely
299 statistical-based response to the meteorological forcing on a per time step basis (Abramowitz, 2005).
300 The purpose of comparison of a conceptual model against ANN output must be clearly understood.

The ANN will always outperform mechanistic, conceptual models because the ANN effectively has up to 100 optimised parameters whereas most conventional models have less than 10. A direct comparison is therefore inappropriate. However, that the ANN does tell us is the information content of the dataset: it indicates whether a model is performing badly because it fails to capture underlying relationships in the data, or whether it is performing badly because the dataset is too noisy. Thus, it offers a statistical evaluation of model performance.

2.8. Filtering the data set

Sapflow data were filtered to avoid division by zero errors by including data only between 0900 h and 1600 h. This excludes hours when solar radiation was zero. To avoid wet-canopy conditions, days with rainfall events were also excluded. This filtered data-set was used to define the boundary conditions for Equations (5, 6, 7a, b). To avoid circularity (using the same data to both parameterise the model and to compare with model outputs), the total 109 day data set spanning the year containing measurements from Jan-Feb, Jun-Jul and Aug-Sep, were partitioned into two separate data sets of alternate days. The first set (days 1, 3, 5 ….) was used to optimise the seasonal response parameters, and the second set (days 2, 4, 6 ….) was used to validate the model. No systematic patterns were evident in the data and there was no change in model outputs when allocation of each half of the data set to either optimisation or validation was reversed.

3. Results

Maximum daily solar radiation ranged from 100 to almost 1400 W m^{-2} in summer and from 100 to 800 W m^{-2} in winter whilst the maximum daily vapour pressure deficit ranged between 0.5 to 7 kPa

325 in summer and 0.1 to 1.6 kPa in winter (Fig. 1a). The Liverpool Plains are characterised by summer
326 dominant rainfall and a drier winter and this was evident during the study period, when there were 19
327 rain events during January and late February and 6 smaller events in July, August and September
328 (Fig. 1b). Summer maximum daily total soil moisture content in the top 60 cm reached 110 mm
329 (18.3 %) after two consecutive rain events during January, with subsequent decreases in E_c resulting
330 from a gradual decline in θ to a minimum of 42 mm (Fig. 1b). During winter maximum total daily θ
331 reached a maximum of 90 mm (Fig. 1b). Mean daily stand transpiration (E_c) varied up to 8-fold on
332 consecutive days. Mean daily stand transpiration measured with the sapflow sensors (scaled by
333 sapwood area) varied from 0.09 mm d^{-1} during a rainy day (24th Feb) up to approximately 2.8 mm d^{-1}
334 (28th Feb) on a rain-free day in summer (Fig. 1c). During winter, E_c varied between no measurable
335 transpiration (E_c << 0.01 mm d^{-1}) on a rainy day (11th Jul) up to 2.08 mm d^{-1} on a rain-free day (28th
336 Jul). Declining E_c between the 4th Feb and 22nd Feb was associated with declining soil moisture
337 content, whilst large increases in E_c occurred after the 13th Jan and after 24th Feb following large rain
338 events and hence soil recharge. An increase in soil moisture was evident from the 1st Aug, and was
339 associated with an increase in stand water use. The three largest rainfall events during the summer
340 period increased soil moisture at 50 cm depth, whereas during winter most rainfall events had little
341 effect on soil moisture at 50 cm depth (Fig. 1b).
342
343 *3.1. Modelled stand water use*
344
345 Five free parameters for g_c^{mod} and six free parameters for E_c^{JS} were optimised by minimising the
346 weighted sum of the square of residuals by using the Differential Evolution genetic algorithm in
347 *Mathematica*©. Results from the genetic algorithm produced a set of maximum likelihood parameters
348 that best describe seasonal responses. Figure (2a, b, c) shows the relationships between E_c and the

driving variables R_s, D and θ and figure (2d, e, f) shows the relationships of g_c against the same driving variables. Generally the functional forms fit well to the boundary regions described by the data, except for the response of E_c to D for the winter (Fig. 2b). The residuals between measured and modelled data (Fig. 3) reveal a minor heteroscedasticity, as evident by the slight pattern of the residuals. In order to properly account for this heterscedascticity, we used a weighting term (Equation (8a). Using this weighting term explained the random errors (ε) in the measurements to be normally distributed, with the 68% confidence interval being within ±1 standard deviation (data not shown). Table 1 contains the best estimates of parameters for Equations (4), (5), (6), (7a) and (7b) along with their respective standard errors. All parameter values were found to be statistically significant (P<0.05).

When applying the PM model, the seasonal response parameters relating to g_c were used in the full form of Equations (3) to derive estimates of canopy conductance (g_c^{mod}) and then in Equation (1) to give estimates of stand water use (E_c^{PM}). Where the modified JS model was applied, the seasonal response parameters for E_c, were used in Equation (4) to derive estimates of stand water use (E_c^{JS}). Figure 4 shows a comparison of E_c estimates from the PM equation (E_c^{PM}) and modified JS (E_c^{JS}) model, against scaled measurements of stand transpiration (E_c^{stand}) and predictions from an ANN over the January-February summer period and July-September winter period. There was a slight under-prediction of E_c^{stand}, using both models, from the 17th-23rd Jan and 25th-29th Feb, which coincides with prior large rain events. Under-prediction of E_c^{stand} was observed throughout the winter period but it was only occasionally seen in the summer. This under-prediction in both cases affects the total daily sums of E_c from both models. The ANN shows a night-time bias in its fitting, resulting in predictions of night-time E_c during both summer and winter periods which are not always

372 measured by the sapflow sensors, especially in winter. The ANN was unable to account for night-
373 time E_c from the 27th-31st July. Points of failure in the fitting seem to be replicated across both models
374 and the ANN. E_c^{JS} is much closer to the ANN in terms of explaining observed variations in E_c.
375
376 To allow a more detailed comparison amongst the ANN and model outputs, changes in hourly rates
377 of stand transpiration for four representative days are presented (Fig. 5). In summer months, the
378 modified JS model and PM model represent the morning trend of increasing sapflow equally well but
379 neither was able to represent the late afternoon/early evening trends in sapflow very accurately. On
380 average, in summer, the modified JS model either slightly (< 10%) underestimated or slightly over-
381 estimated midday rates of stand transpiration, whilst the PM model either closely matched or
382 underestimated by a larger margin (15%) midday rates of stand transpiration. The ANN consistently
383 followed the changes in transpiration rate more closely throughout the 24 h period.
384
385 The performance of both models was less satisfactory in winter than summer (Fig. 5). The PM model
386 consistently underestimated the rate of stand transpiration, particularly in the morning, but over
387 estimated transpiration in the afternoon on some days. The modified JS model performed better than
388 the PM model in winter by a better representation of the maximum rates of transpiration. However it
389 failed to adequately represent the early morning increase in transpiration observed in the data. As
390 expected the ANN most closely matched the daily trends of transpiration.
391
392 The sapflow sensors measured a total of 75.4 mm of transpiration by the canopy for the 109 day
393 study period between 0900 h and 1600 h. All three models gave a similar sum: the modified JS sum
394 for 109 days was 84 mm; for the PM model the sum was 75 mm; the ANN sum was 76.4 mm.
395

Regression analysis revealed strong linear relationships between measured and modelled rates of stand water use (Fig. 6). In all cases the slope of the regression for summer data was closer to one than the slope for the winter data, which was always significantly less than one. Furthermore, in all cases the goodness-of-fit for the summer data was better than for the winter data. Thus, slopes of 0.86 and 0.79 for E_c^{JS} and E_c^{PM} respectively were observed and E_c^{JS} explained 87% of the variance and E_c^{PM} explained 86%. The ANN gave a slope of 0.85 and explained 86% of the variance.

4. Discussion

The responses of canopy conductance (PM model) and stand water use (modified JS model) (Fig. 2) to each abiotic driving variable agree well with responses observed previously in a range of different forest types (Zhang et al., 1997; Sommer et al., 2002; Silberstein et al., 2003; Harris et al., 2004; Komatsu et al., 2006b; Fig. 8). Values for $E_{c,max}$, $g_{c,max}$, k_1, k_3, θ_w and θ_c (Table 1) also compare well with previous studies (Harris et al., 2004; Komatsu et al., 2006b). The estimated value for $E_{c,max}$ of 0.267 mm hr^{-1} from the modified JS model is comparable to the measured maximal value of 0.280 mm hr^{-1}. However, the estimated value of 0.0082 mm s^{-1} for $g_{c,max}$ from the PM model is significantly over-estimated compared to the measured value (0.0058 mm s^{-1}). The reason why the modelled estimate of $g_{c,max}$ is larger than the measured value is because the maximum value of E_c occurs in the mid-range of D (Fig. 2b) but the modelled $g_{c,max}$ predicts maximum values under conditions of low D and high R_s (Fig 2c, d) and such conditions do not occur in the field. Consequently there are no (large) values for observed $g_{c,max}$ corresponding to these modelled environmental conditions. This also means that the modified JS model is easier to fit than the PM model. However, this overestimation of $g_{c,max}$ had little impact on hourly values of E_c because of good agreement between

419 modelled and measured hourly values of g_c. However, E_c^{PM} under-predicted, to a greater degree
420 (especially in winter) the measured values of transpiration when compared with E_c^{JS} because of the
421 poor ability of E_c^{PM} to account for the impact of the generally lower soil moisture content in winter.
422 Additionally, the value of $g_{c,max}$ may be too low for the model (despite being higher than the
423 measured value). Consequently for the PM equation to better predict E_c, the required value for
424 modelled $g_{c,max}$ would need to be much higher.
425
426 As R_s increases, g_c and E_c increase asymptotically from zero to a maximum. At low levels of incident
427 radiation, energy supply limits evaporation, but at high levels of radiation, other factors (especially
428 soil moisture content and hydraulic conductance of soil and plant), limit evapotranspiration (Williams
429 et al., 1998). The boundary curves for R_s show that both the E_c and g_c responses are almost identical
430 and provide a good description of the asymptotic increase of E_c and g_c with increasing R_s.
431
432 We found that incorporating the soil moisture response function was critical for the model to
433 satisfactorily describe variations in E_c and g_c, especially under limiting soil water conditions. Such a
434 conclusion has been made previously (Wright et al., 1995; Harris et al., 2004). The observed patterns
435 in the response of E_c and g_c to θ compares well with those found by Kelliher et al. (1993), Harris et
436 al. (2004) and Komatsu et al. (2006b) and is attributed to the impact of a declining θ on stomatal, and
437 hence canopy, conductance (Eamus et al., 2006, Zeppel et al., 2008) and the need to avoid
438 excessively low leaf water potentials and hence xylem cavitation (Thomas and Eamus 1999).
439
440 In contrast to the relatively simple relationship linking θ and E_c and g_c, the relationship between E_c, g_c
441 and D was more complex. The functional responses of E_c and g_c to D differ because the response of
442 E_c to D is determined by both the direct response of stomata to D (or rather, transpiration rate; Mott

443 and Parkhurst, 1991; Monteith, 1995; Eamus et al., 2008) and the response of diffusion *per se* to *D*.
444 The response of g_c to increasing *D* compares well with other studies that have found an exponential
445 response (e.g. Granier and Loustau, 1994; Wright et al., 1995; Harris et al., 2004). The three-phase
446 behaviour of stand water use is comparable to that of stomatal behaviour observed at the leaf
447 (Monteith, 1995; Thomas and Eamus, 1999; Eamus and Shanahan, 2002) and canopy scales
448 (Komatsu et al., 2006b; Zeppel, 2006) and is the result of a feedback between increasing cuticular
449 water loss as *D* increases and a declining supply of water to guard cells (Eamus et al., 2008). The
450 initial response of E_c for low values of *D* is unlikely to be a response to the covariance of R_s in the
451 morning, because even under a constant saturating level of light, the same three-phase behaviour was
452 observed (Thomas and Eamus, 1999). The threshold of 2–3 kPa for the transition to declining
453 transpiration with increasing *D* observed in the present study is larger than that observed by Pataki
454 and Oren (2003) and Komatsu et al. (2006b) and the decline in E_c was more severe than the decline in
455 g_c they observed. This difference is probably because the site used in the present study is much drier,
456 experiences a much larger range of *D* (as high as 7 kPa) and was recovering from a long period of
457 drought, compared to those used by Pataki and Oren (2003) or Komatsu et al. (2006b). The response
458 of stomata (and hence water use) to *D* is strongly influenced by soil moisture content (Thomas and
459 Eamus, 1999; Thomas et al., 2000) and therefore the long-term (> 4 y) drought experienced at the
460 present site is likely to have influenced the response we observed.
461
462 Daily variations in E_c^{stand} were captured well by both the modified JS and PM models. Observed
463 hourly stand water use varied 12 fold over a period of one week in mid-January and the model was
464 able to replicate this range and the time course of the response of stand water use to fluctuations in
465 solar radiation, *D* and soil moisture. Similarly, more gradual declines in the maximum rate of stand
466 water use that were observed during drying periods (late Jan to late Feb) were captured in the models

as well as the drier periods in winter. Poor model performance was generally seen during and immediately after large rainfall events, where large increases in observed rates of stand transpiration (15th -17th Jan and 27th-31st Jul) were not captured by the models. This could be because the sapflow sensors, located at the base of the tree stem, were measuring a significant volume of canopy recharge in the absence of significant rates of transpiration (because of low values of R_s and D). Such recharge is driven by gradients of water potential between soil and leaf (Dawson et al., 2007), which were large in the present study but neither model incorporate such a mechanism for driving water flux up the stem. Similarly the presence of nocturnal flows on several nights (for example, January 14th to January16th, February 25th to February 27th and July 28th to July 30th) were not captured by either model as both models assume stomatal closure at night. A simple calculation can estimate the potential contribution of canopy recharge to these two issues. The basal area of the two dominant tree species is 20.4 m^2 ha^{-1}. Average bole height of these two species is approximately 10 m so the total stem volume (ignoring branches and wood in the canopy) is 204 m^3 ha^{-1}. The average water content of the sapwood for the two species is 37.5 % (Zeppel et al., 2004) and we assume that the daily fluctuation in water content resulting from depletion and recharge of stem storage is no more than 50 % of this. Therefore a maximum of 38.25 m^3 ha^{-1} of stored water is available. Rates of nocturnal flow range from 0.5 mm ha^{-1} night^{-1} (25th/26th February) to 1 mm ha^{-1} night^{-1} (14th/15th January), or 5 m^3 to 10 m^3 ha^{-1} night^{-1}. This value compares favourably with the estimated maximum volume of water that may be discharged and recharged in one night (38.25 m^3 ha^{-1}).

Nocturnal flows were not observed on every night and were most commonly observed after significant rain had wet the soil profile. When this occurs, the gradient of water potential between soil and canopy is increased, the soil-to-root hydraulic connectivity is increased and nocturnal atmospheric humidity is generally increased. Such conditions favour canopy recharge (Dawson et al.,

2007). If the hydraulic conductivity of the soil-plant transport pathway is 2.0 mmol m^{-1} s^{-1} (Zeppel, 2006) and the gradient in water potential is 1.0 MPa, then the maximum volume of recharge that can occur in a single 10 h night is 12.96 m^3 ha^{-1} $night^{-1}$, a value that agrees well with the estimated range of nocturnal flows (5 – 10 m^3 ha^{-1} $night^{-1}$). It would appear that canopy recharge is a very large fraction (up to 100 %) of the nocturnal flow observed and nocturnal transpiration through open stomata is therefore a small fraction of the total sapflow measured at nigh with sapflow sensors located at the base of the stem.

To compare daily performance of the models in more detail we consider a sampling of 2 days from the summer and winter periods (Fig. 5). Differences between the modified JS model and PM model in summer were marginal and both follow a trend similar to the ANN. In winter, however, the performance of the PM model dropped significantly with an underestimation of up to 50% during daylight hours. The modified JS model reduced this underestimation to less than 20% and compares well against the ANN. There was also a bias towards over-estimates of sapflow in the afternoon for both models in winter, which the ANN did not exhibit.

The outputs of both models in winter lagged the observed values in the morning or morning and afternoon (Fig 5). The relative failure of the JS model to fit to some days in winter appears to be because of the large number of winter data values which lie to the left (that is, outside) of the boundary line defined by equation 8b (Fig. 2b). The boundary line defines the boundary well for summer data but fails to define the boundary in winter and this leads to the lag between model and measurement on some winter days. A slight but significant improvement in fit (reducing the time lag between JS and observed rates of sapflow) of the modified JS model was produced if the model, when applied to the winter period, used parameter values derived only from winter data, rather than

parameterising with the entire data set (data not shown). Failure to accurately predict E_c by the models during some of these winter days was not due to the data set being too small, as the ANN was able to accurately replicate all daily patterns (include night time fluxes) across both seasons. On a statistical basis, variations in R_s, D and θ are measured with sufficient frequency and resolution to account for observed changes in E_c.

The effect of temperature on E_c was also investigated. However, we found that incorporating temperature in either the PM or JS models had a negative impact on model performance and increased the error in the seasonal response parameters. Consequently the temperature response function was omitted. Similar problems in the use of a temperature function were found by Wright et al. (2005) and Sommer et al. (2002).

The modified JS model was applicable to conditions of low and high E_c in summer at hourly time-steps with a slope of the regression of model *versus* observed values of 0.92. In winter, the modified JS performed less well when E_c was large. In both summer and winter the PM model performed less well than the JS at both low and high rates of E_c (Fig 5) and therefore at short timeframes (hourly) the JS was generally more applicable than the PM model, which appears to be less successful under conditions of low E_c at hourly time-steps in some studies (David et al., 1997; Rana et al., 2005) or less successful under conditions of high E_c in the present study (Fig. 5)

The sum of water used between 0900 h and 1600 h across the entire 109 day period was 75.4 mm. The PM model predicted a 109 day sum of 75 mm and the modified JS model predicted 84mm whilst the ANN model predicted 111 mm. The ANN model has a very large number of parameters and is expected to fit the data extremely well because the size of the data set was sufficiently large to allow

539 this. In summer the fit of the modified JS data to experimental data was very good (Fig. 6) and
540 despite the poorer fit in winter on some days because of the poor definition of the winter boundary
541 values for the response function for *D*, the 109 day sum of water used derived from the modified JS
542 model was very close to the actual sum of water used. It is apparent that despite limitations of both
543 the PM and JS models on some days under some conditions, at hourly time-steps (Figs 5, 6) the
544 aggregate behaviour over a sufficient number of days (Fig. 6) results in a close agreement between
545 observed and modelled total sums of water transpired.

546 **5. Conclusions**

547

548 For this study we have used a standard (*via* an inversion of the PM equation) and a modified JS (*via*
549 direct modelling of transpiration rate) approach to model the responses of stand-scale transpiration
550 and canopy conductance to changes in solar radiation, vapour pressure deficit and soil moisture
551 content. We were able to *parameterise* both models using a limited number of sapflow measurements
552 and corresponding environmental driving variables over 55 days, incorporating data from both
553 summer and winter periods. Model response functions for canopy conductance and stand
554 transpiration were found to describe variation in E_c due to solar radiation, vapour pressure deficit and
555 soil moisture content. These responses compared well with those found in previous studies on
556 different forest types. Both models performed equally well during summer when soil water content
557 was fairly high. During winter the modified Jarvis model performed significantly better than the
558 Penman-Monteith model, especially under conditions of high transpiration. However, over the entire
559 109 day study period the total modelled daytime sums of water used were all very close to the
560 observed sum of 75.4 mm.

561

562

Acknowledgements

Weather data were provided by the NSW Department of Agriculture. This project was conducted in collaboration with the State Forests of New South Wales and the NSW Department of Agriculture. We thank the Cudmore family for providing access to their property (Paringa). Funding was provided by the CRC for Greenhouse Accounting and the Australian Research Council. We also thank Gab Abramowitz for his help in applying SOLO for our ANN analysis, and in extension Kuo-lin Hsu for providing the SOLO code.

References

Abramowitz, G., 2005. Towards a benchmark for land surface models. Geophys. Res. Lett. 32.

Banks, R., 1998. Soil landscapes of the Blackville 1:1000 000 sheet. Department of Land and Water Conservation, Gunnedah.

David, T.S., Ferreira, M.I., David, J.S., Pereira, J.S., 1997. Transpiration from a mature *Eucalyptus globulus* plantation in Portugal during a spring–summer period of progressively higher water deficit. Oecologia. 110, 153–159.

Dawson, T.E., Burgess, S.S.O., Tu, K.P., Oliveira, R.S., Stantiago, L.S., Fisher, J.B., Simonin, K.A., Ambrose, A.R., 2007. Nighttime transpiration in woody plants from contrasting ecosytems. Tree Physiol. 27, 561-576.

Dolman, A.J., Gash, J.H.C., Roberts, J., Shuttleworth, W. J., 1991. Stomatal and surface conductance of tropical rainforest. Agric. For. Meteorol. 54, 303-313.

586 Eamus, D., Shanahan, S., 2002. A rate equation model of stomatal responses to vapour pressure
587 deficit and drought. BMC Ecology. 2, 1-14.
588 Eamus, D., Hatton, T.J., Cook, P.G., Colvin, C., 2006. 'Ecohydrology: vegetation function, water and
589 resource management.' CSIRO: Melbourne. pp. 361.
590 Eamus, D., Taylor, D.T., Macinnis-Ng, C.M., Shanahan, S., De Silva, L., 2008. Comparing model
591 predictions and experimental data for the response of stomatal conductance and guard cell
592 turgor to manipulations of cuticular conductance, leaf-to-air vapour pressure difference and
593 temperature: feedback mechanisms are able to account for all observations. Plant Cell
594 Environ. 31, 269-277.
595 Ewers, B.E., and Oren, R., 2000. Analyses of assumptions and errors in the calculation of stomatal
596 conductance from sap flux measurements. Tree Physiol. 20, 579 - 589.
597 Ewers, B.E., Mackay, D.S., Samanta, S., 2007. Interannual consistency in canopy stomatal
598 conductance control of leaf water potential across seven tree species. Tree Physiol. 27, 11-24.
599 Gash, J.H.C., Shuttleworth, W.J., Lloyd, C.R., Andre, J.C., Goutorbe, J.P., Gelpe, J., 1989.
600 Micrometeorological measurements in Les Landes forest during HAPEX-MOBILHY. Agric.
601 For. Meteorol. 46, 131-147.
602 Goldberg, D.E., 1989. Genetic Algorithms in Search, Optimization, and Machine Learning. Addison-
603 Wesley Professional, London.
604 Granier, A., Loustau, D., 1994. Measuring and modelling the transpiration of a maritime pine canopy
605 from sap-flow data. Agric. For. Meteorol. 71, 61-81.
606 Granier, A., Huc, R., Barigah, S.T., 1996. Transpiration of natural rain forest and its dependence on
607 climatic factors. Agric. For. Meteorol. 78, 19–29.
608 Granier, A., Biron, P., Leoine, D., 2000. Water balance, transpiration and canopy conductance in two
609 beech stands. Agric. For. Meteorol. 100, 291-308.

610 Harris, P.P., Huntingford, C., Coxb, P.M., Gash, J.H.C., Malhi, Y., 2004. Effect of soil moisture on
611 canopy conductance of Amazonian rainforest. Agric. For. Meteorol. 122, 215–227.
612 Hsu, K., Gupta, H.V., Gao, X., Sorooshian, S. and Imam, B., 2002. Self-organizing linear output map
613 (SOLO): An artificial neural network suitable for hydrologic modelling and analysis. Water
614 Resour. Res. 38, 1-17.
615 Hutley, L.B., O'Grady, A.P., Eamus, D., 2001. Monsoonal influences on evapotranspiration of
616 savanna vegetation of northern Australia. Oecologia. 126, 434-443
617 Jarvis, P.G., 1976. The interpretation of the variations in leaf water potential and stomatal
618 conductance found in canopies in the field. Phil. Trans. R. Soc. Lond. B. 273, 593-610.
619 Jarvis, P.G., McNaughton, K.G. 1986. Stomatal control of transpiration: scaling up from leaf to
620 region. Adv. Ecol. Res. 15, 1-49.
621 Kelliher, F.M., Leuning, R., Schulze, E.D., 1993. Evaporation and canopy characteristics of
622 coniferous forests and grasslands. Oecologia. 95, 153-163.
623 Kirkup, L., Foot, M., Mulholland, M., 2004. Comparison of equations describing band broadening in
624 high-performance liquid chromatography. J. Chromatogr. A.1030, 25-31.
625 Kohonen, T., 1989. Self-Organising and Associative Memory. Springer, New York.
626 Komatsu, H., Kang, Y., Kume, T., Yoshifuji, N., Hotta, N., 2006a. Transpiration from a *Cryptomeria*
627 *japonica* plantation, part 1: aerodynamic control of transpiration. Hydrol. Process. 20, 1309-
628 1320.
629 Komatsu, H., Kang, Y., Kume, T., Yoshifuji, N. Hotta, N., 2006b. Transpiration from a *Cryptomeria*
630 *japonica* plantation, part 2: responses of canopy conductance to meteorological factors.
631 Hydrol. Process. 20, 1321-1334.

632 Kosugi, Y., Takanashi, S., Tanaka, H., Ohkubo, S., Tani, M., Yano, M., Katayama, T., 2007.
633 Evapotranspiration over a Japanese cypress forest. I. Eddy covariance fluxes and surface
634 conductance characteristics for 3 years. J. Hydrol. 337, 269-283.
635 Lagergren, F. and Lindroth, A., 2002. Transpiration response to soil moisture in pine and spruce trees
636 in Sweden. Agric. For. Meteorol. 112, 67-85.
637 Lu, P., Yunusa, I.A.M., Walker, R.R., Muller, W.J., 2003. Regulation of canopy conductance and
638 transpiration and their modelling in irrigated grapevines. Funct. Plant Biol. 30, 689-698.
639 Medhurst, J.L., Battaglia, M., Beadle, C.L., 2002. Measured and predicted changes in tree and stand
640 water use following high intensity thinning of an 8 year old *E. nitens* plantation. Tree Physiol.
641 22, 775–784
642 Monteith, J.L., 1965. Evaporation and Environment. Sym. Soc. Exp. Biol. 19, 205-204.
643 Monteith, J.L., 1995. A reinterpretation of stomatal responses to humidity. Plant Cell Environ. 18,
644 357-364.
645 Mott, K.A., Parkhurst, D.F., 1991. Stomatal responses to humidity in air and helox. Plant Cell
646 Environ. 14, 509-515.
647 O'Grady, A.P., Eamus, D. Hutley, L.H., 1999. Transpiration increases in the dry season: patterns of
648 tree water use in the eucalypt open forests of northern Australia. Tree Physiol. 19, 591-597.
649 O'Grady, A.P., Eamus, D., Cook, P.G., Lamontagne, S., 2006. Groundwater use by riparian
650 vegetation in the wet-dry tropics of northern Australia. Aust. J. Bot. 54, 145-154.
651 Ogink-Hendriks, M.J., 1995. Modelling surface conductance and transpiration of an oak forest in The
652 Netherlands. Agric. For. Meteorol. 74, 99-118.
653 Pataki, D.E., Oren, R., 2003 Species differences in stomatal control of water loss at the canopy scale
654 in a mature bottomland deciduous forest. Adv. Water Resour. 26, 1267-1278.

655 Rana, G., Katerji, N., de Lorenzi, F., 2005. Measurement and modelling of evapotranspiration of
656 irrigated citrus orchard under Mediterranean conditions. Agric. For. Meteorol. 128, 199-209.
657 Rollenbeck, R., Dieter, A., 2007. Characteristics of the water and energy balance in an Amazonian
658 lowland rainforest in Venezuela and the impact of the ENSO-cycle. J. Hydrol. 337, 377-390.
659 Silberstein, R.P., Sivapalan, M., Viney, N.R., Held, A., Hatton, T.J., 2003. Modelling the energy
660 balance of a natural jarrah (*Eucalyptus marginata*) forest. Agric. For. Meteorol. 115, 201-230.
661 Simonin, K., Kolb, T.E., Montes-Helu, M., Koch, G.W., 2007. The influence of thinning on
662 components of stand water balance in a ponderosa pine forest stand during and after extreme
663 drought. Agric. For. Meteorol. 143, 266-276.
664 Sommer, R., de Abreu Sa, T.D., Vielhauer, K., de Araujo, A.C., Folster, H., Vlek, P.L.G., 2002.
665 Transpiration and canopy conductance of secondary vegetation in the eastern Amazon. Agric.
666 For. Meteorol. 112, 103-121.
667 Stewart, J.B., 1988. Modelling surface conductance of pine forest. Agric. For. Meteorol. 43, 19-35.
668 Thomas, D.S., Eamus, D., 1999. The influence of predawn leaf water potential on stomatal responses
669 to atmospheric water content at constant C_i and on stem hydraulic conductance and foliar
670 ABA concentrations. J. Exp. Bot. 50, 243-251.
671 Thomas, D.S., Eamus, D., Shanahan, S., 2000. Influence of season, drought and xylem ABA on
672 stomatal responses to leaf-to-air vapour pressure difference of trees of the Australian wet-dry
673 tropics. Aust. J. Bot. 48, 143-151.
674 Whitehead, D., 1998. Regulation of stomatal conductance and transpiration in forest canopies. Tree
675 Physiol .18, 633–644.
676 Whitley, R.J., Zeppel, M.J.B., Armstrong, N., Macinnis-Ng, C., Yunusa, I.A.M., Eamus, D., 2008. A
677 modified JS model for predicting stand-scale transpiration of an Australian native forest. Plant
678 and Soil. 305, 35-47.

679 Williams, M., Malhi, Y., Nobre, A., Rastetter, E., Grace, J. Pereira, M., 1998. Seasonal variation in
680 net carbon exchange and evapotranspiration in a Brazillian rain forest. Plant Cell Environ. 21,
681 953-968.
682 Wright, I.R., Manzi, A.O., da Rocha, H.R., 1995. Surface conductance of Amazonian pasture: model
683 application and calibration for canopy climate. Agric. For. Meteorol. 75, 51-70.
684 Wullschleger, S.D., Hanson, P.J., 2006. Sensitivity of canopy transpiration to altered precipitation in
685 an upland oak forest: evidence from a long-term field manipulation study. Glob. Change.
686 Biol. 12, 97-109.
687 Wullschleger, S.D., Hanson, P.J., Todd, D.E., 2001. Transpiration from a multi-species deciduous
688 forest as estimated by xylem sapflow techniques. Forest Ecol. Manag. 143, 205-213.
689 Yunusa, I.A.M., Walker, R.R., Loveys, B.R. Blackmore, D.H., 2000. Determination of transpiration
690 in irrigated grapevines: Comparison of the heat-pulse technique with gravimetric and
691 micrometeorological methods. Irrigation Sci. 20, 1-8.
692 Zeppel, M.J.B., 2006 The influence of drought and other abiotic factors on tree water use in a
693 temperate remnant forest. PhD Thesis. University of Technology Sydney.
694 Zeppel, M.J.B., Macinnis-Ng, C., Yunusa, I.A.M., Whitley, R.J., Eamus, D., 2008. Long term trends
695 of stand transpiration in a remnant forest during wet and dry years. J. Hyrdol. 349, 200-213.
696 Zeppel, M.J.B., Eamus, D., 2008 Coordination of leaf area, sapwood area and canopy conductance
697 leads to species convergence of tree water use in a remnant evergreen woodland. Aust. J. Bot.
698 56, 97-108.
699 Zeppel, M.J.B., Murray, B.R., Barton, C. Eamus, D., 2004. Seasonal responses of xylem sap velocity
700 to VPD and solar radiation during drought in a stand of native trees in temperate Australia.
701 Funct. Plant Biol. 31, 461-470.

Zhang, H., Simmonds, L.P., Morison, J.I.L., Payne, D., Wullschleger, S.D., 1997. Estimation of transpiration by single trees: comparison of sapflow measurements with a combination equation. Agric. For. Meteorol. 87, 155-169.

Fig. 1: a) Daily averages of incident solar radiation (R_S), 0900 h vapour pressure deficit values (D), b) total soil moisture content to a depth of 60 cm (θ), daily rainfall and c) total daily stand transpiration (E_c) for the periods of January, February, July and September 2004. Diurnal changes in the three driving environmental variables R_S, D and θ show resulting variations in E_c.

Fig. 2: The functional dependencies based on the optimised parameters of stand transpiration on (a) hourly solar radiation, (b) vapour pressure deficit and (c) soil moisture content at 50 cm; and canopy conductance on (d) hourly solar radiation, (e) vapour pressure and (f) soil moisture content at 50 cm. The left y-axis represent the scatter of data points and the right y-axis is the normalised fit of the functional forms. Summer and winter values are presented separately for comparative purposes.

Fig. 3: Standardised residuals for (a) the modified JS model and (b) their distribution of error; the standardised residuals for (c) the PM equation and (d) their distribution of error. The dashed lines show the regions for which the residuals fall between ±1 standard deviations, representative of the 68% confidence region. Both models conform to the assumption of a normally distributed error about a mean 0 and standard deviation 1.

Fig. 4: Stand transpiration measured with sapflow sensors (E_{stand}, data points) and estimated stand transpiration from the modified Jarvis-Stewart model (JS, black line), the Penman-Monteith equation (PM, grey line), and artificial neural network (ANN, dotted line) over the sampling periods in a) January, b) February, c) July and d) September 2004.

Fig. 5: Daily variation in stand transpiration measured with sapflow sensors (E_{stand}, points) and modelled with the modified Jarvis-Stewart model (JS, black line), the Penman-Monteith equation (PM, grey line) and the artificial neural network (ANN, dotted line) for a) 20th January, b) 7th February, c) 21st July and d) 6th September 2004.

Fig. 6: Summer (grey circles) and summer (white diamonds) comparisons between measured and modelled stand transpiration from a) modified JS model, b) PM equation and c) ANN.

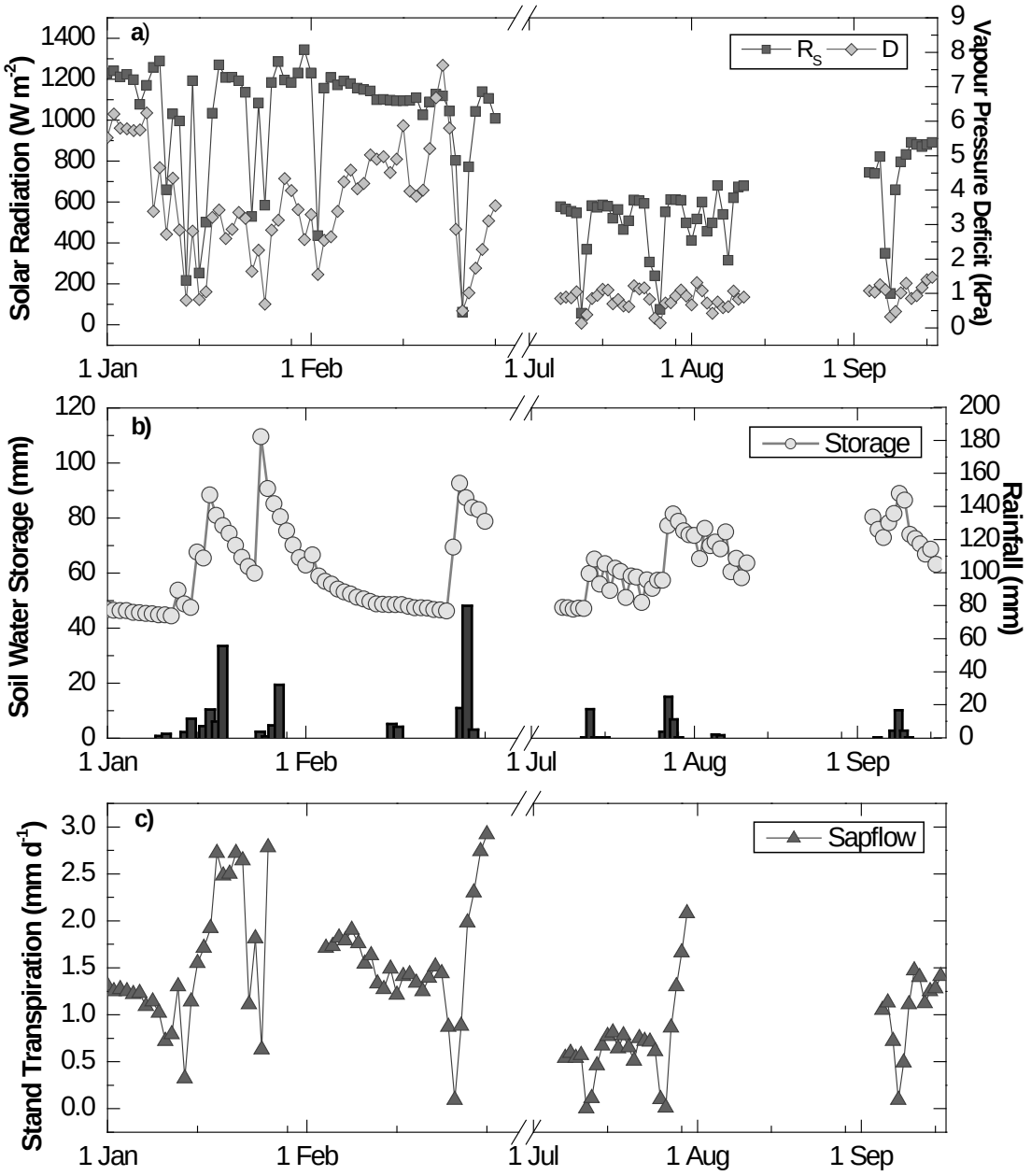
a)
Solar Radiation (W m-2)
Vapour Pressure Deficit (kPa)
Rs
D
1400
1200
1000
800
600
400
200
0
9
8
7
6
5
4
3
2
1
0
1 Jan
1 Feb
1 Jul
1 Aug
1 Sep
b)
Soil Water Storage (mm)
Rainfall (mm)
Storage
120
100
80
60
40
20
0
200
180
160
140
120
100
80
60
40
20
0
1 Jan
1 Feb
1 Jul
1 Aug
1 Sep
c)
Stand Transpiration (mm d-1)
Sapflow
3.0
2.5
2.0
1.5
1.0
0.5
0.0
1 Jan
1 Feb
1 Jul
1 Aug
1 Sep

739

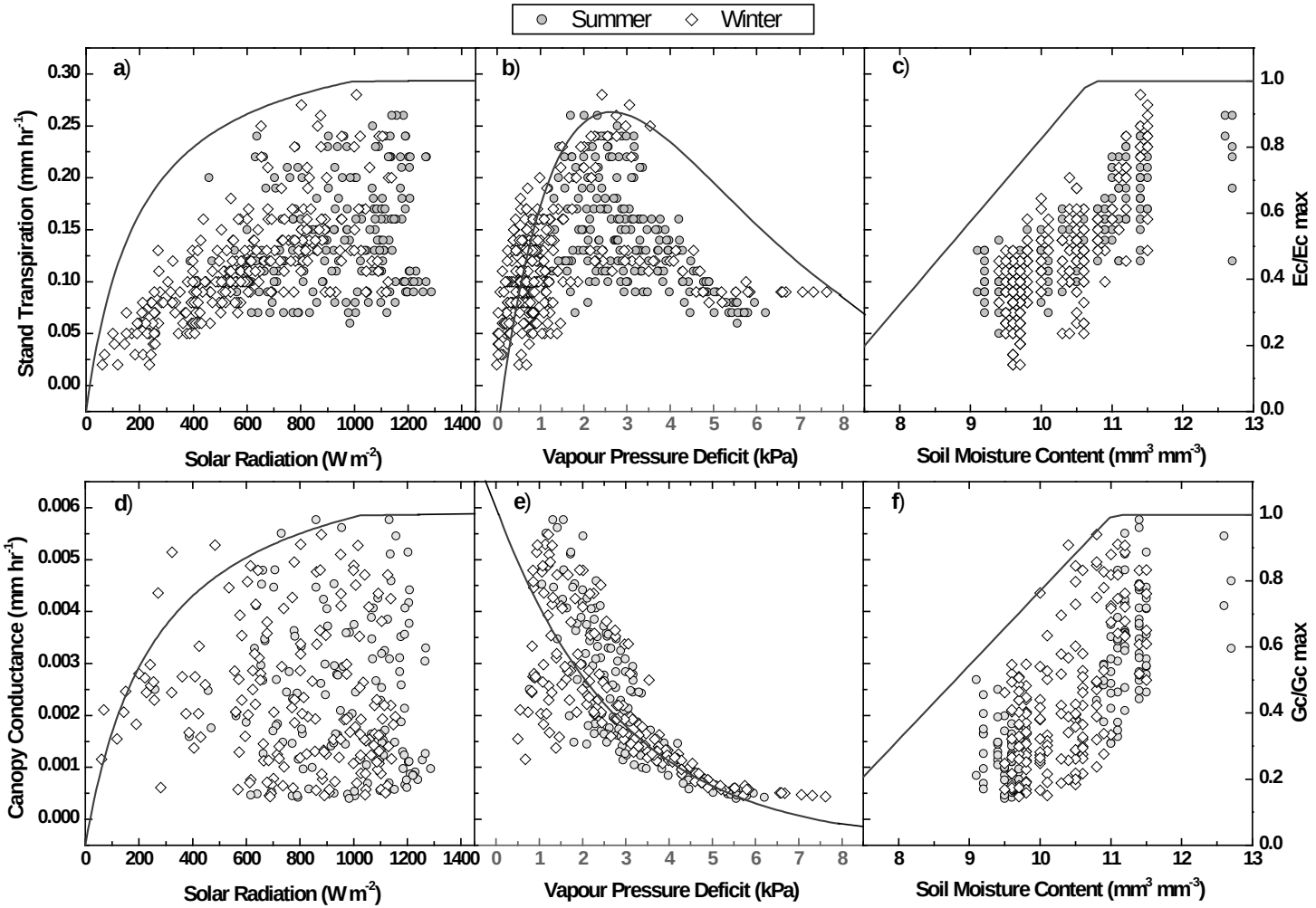
Summer
Winter
a)
b)
c)
d)
e)
f)
Stand Transpiration (mm hr-1)
Canopy Conductance (mm hr-1)
Solar Radiation (W m-2)
Vapour Pressure Deficit (kPa)
Soil Moisture Content (mm3 mm-3)
Ec/Ec max
Gc/Gc max

740

741

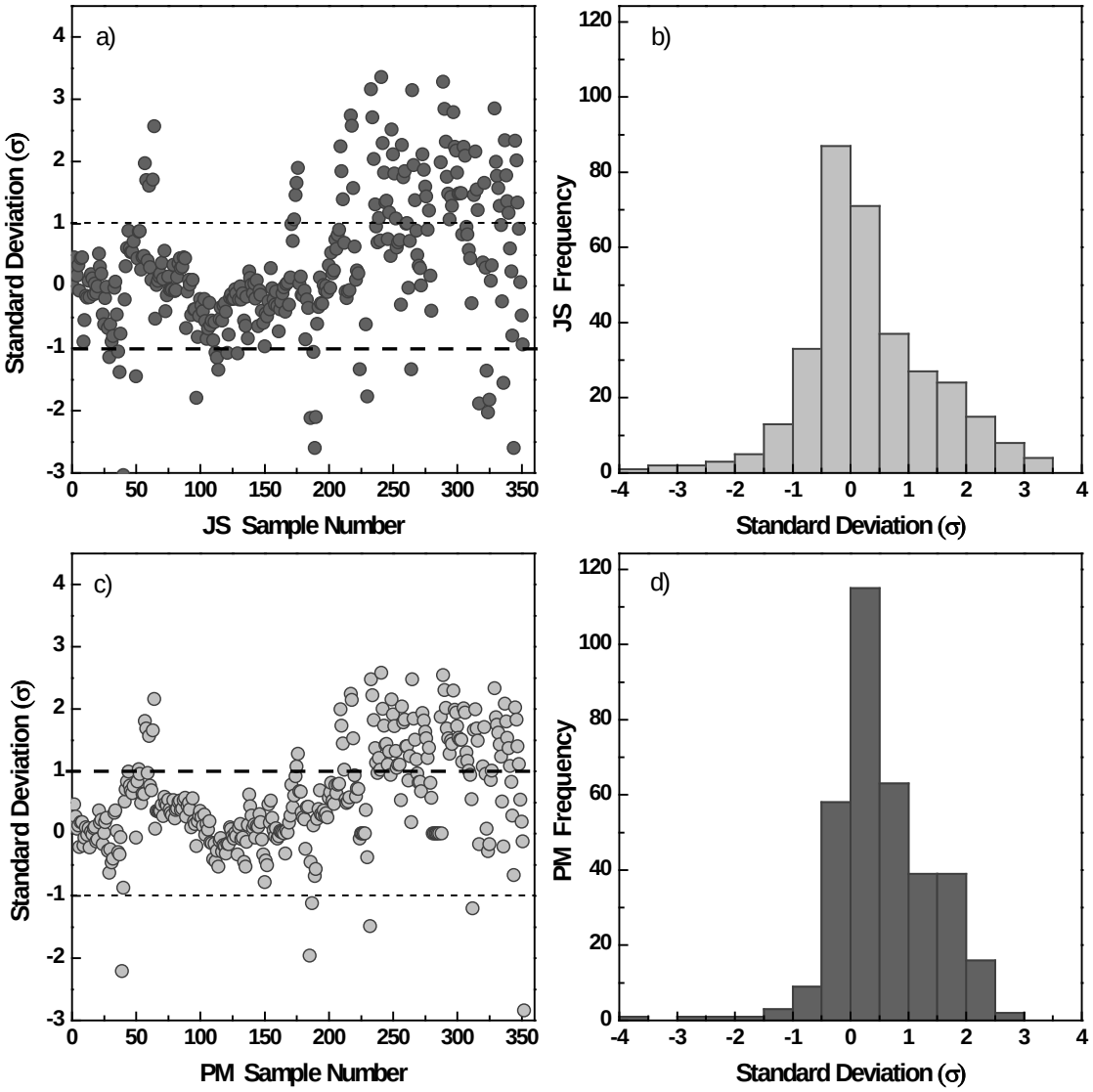

742

743

744

745

746

747

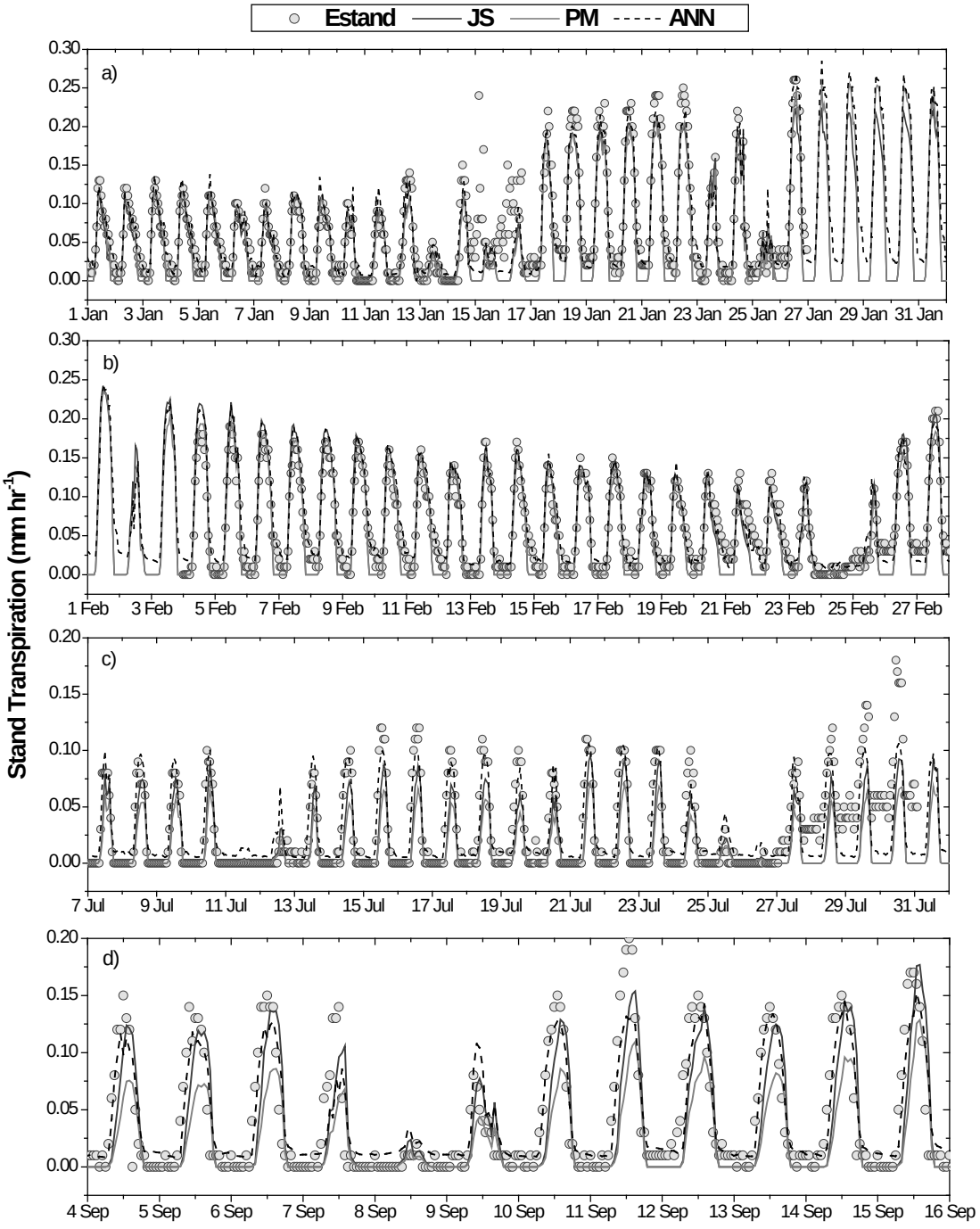
Estand
JS
PM
ANN
a)
b)
c)
d)
Stand Transpiration (mm hr-1)
0.30
0.25
0.20
0.15
0.10
0.05
0.00
1 Jan 3 Jan 5 Jan 7 Jan 9 Jan 11 Jan 13 Jan 15 Jan 17 Jan 19 Jan 21 Jan 23 Jan 25 Jan 27 Jan 29 Jan 31 Jan
1 Feb 3 Feb 5 Feb 7 Feb 9 Feb 11 Feb 13 Feb 15 Feb 17 Feb 19 Feb 21 Feb 23 Feb 25 Feb 27 Feb
7 Jul 9 Jul 11 Jul 13 Jul 15 Jul 17 Jul 19 Jul 21 Jul 23 Jul 25 Jul 27 Jul 29 Jul 31 Jul
4 Sep 5 Sep 6 Sep 7 Sep 8 Sep 9 Sep 10 Sep 11 Sep 12 Sep 13 Sep 14 Sep 15 Sep 16 Sep

748

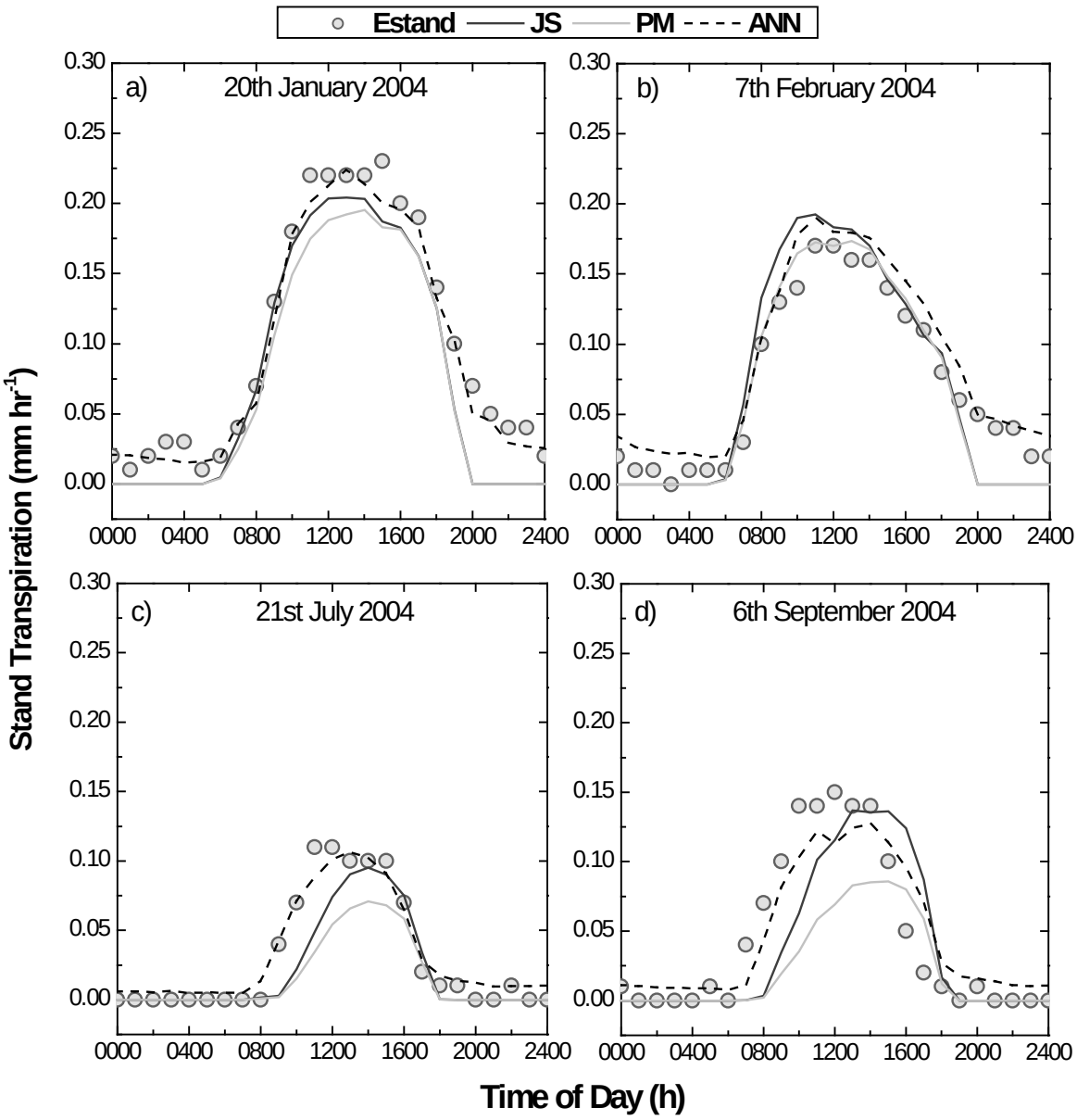
Estand
JS
PM
ANN
a)
20th January 2004
b)
7th February 2004
c)
21st July 2004
d)
6th September 2004
Stand Transpiration (mm hr-1)
Time of Day (h)
0.00
0.05
0.10
0.15
0.20
0.25
0.30
0000
0400
0800
1200
1600
2000
2400

749

750

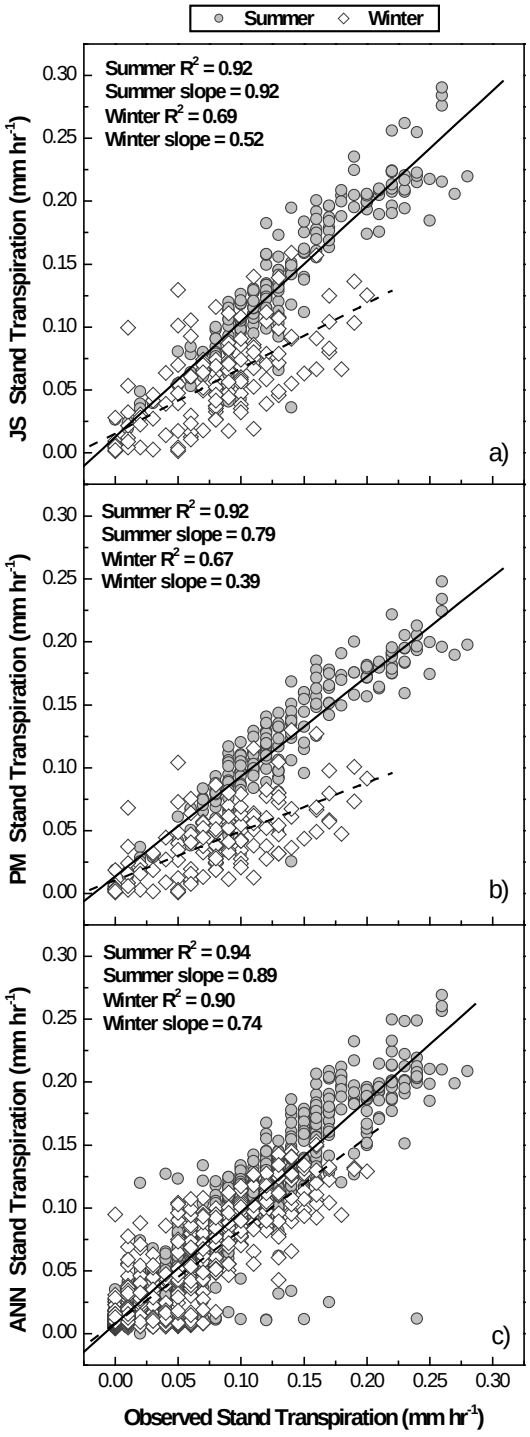

751

752

753

754

Table 1: Parameter estimations for the seasonal response terms, resulting from an optimisation of the traditional and modified Jarvis model using a genetic algorithm. Parameters defined here are both maximum reference values ($\underline{ref_{max}}$) for $g_{c.max}$ and $E_{c.max}$, environmental functional dependencies on solar radiation (k_1), vapour pressure deficit (k_2 and k_3), and soil moisture content at wilting (θ_W), and critical points (θ_C), the constant of proportionality associated with error (β) and explained variance (R^2). Standard errors are given in brackets next to each value.

	E_c^{JS}	g_c^{mod}
ref_{max} (mm hr^{-1})	0.2667(0.0054)	0.00821(0.00012)
k_1 (W m^{-2})	200.38(39.67)	257.99(47.76)
k_2 (kPa)	-	1.08(0.02)
k_3 (kPa)	0.44(0.04)	0.39(0.01)
θ_W (%)	7.0	7.14(0.12)
θ_C (%)	11.84(0.10)	11.49(0.07)
β	0.29	0.38
R^2	0.87	0.86